

EXPERIMENT ON MULTIPACTOR SUPPRESSION IN DIELECTRIC-LOADED ACCELERATING STRUCTURES WITH A SOLENOID FIELD*

C. Jing[#], R. Konecny, A. Kanareykin, S. Antipov, P. Schoessow, Euclid Techlabs LLC, Solon, OH 44139, U.S.A.

C. Chang, L. Xiao, L. Ge, SLAC, Menlo Park, CA, 94309, U.S.A.

M. Conde, J.G. Power, W. Gai, ANL, Argonne, IL 60439, U.S.A.

S. Gold, Naval Research Laboratory, Washington DC, 203751, U.S.A.

Abstract

Efforts by numerous institutions have been ongoing over the past decade to develop a Dielectric-Loaded Accelerating (DLA) structure capable of supporting high gradient acceleration when driven by an external rf source. Multipactor is the major issue limiting the gradient that was revealed in earlier experiments. A theoretical model predicts a solenoid field within an optimal range of field strengths and applied to DLA structures may completely block the multipactor. To demonstrate this approach, an alumina based DLA structure was built and tested. We observed multipactor being successfully suppressed in the straight section of DLA structure with a certain strength of the solenoid field but enhanced in the dielectric taper, which is used for matching impedance in this particular design. Theoretical modeling and numerical simulation match with the experimental results well.

INTRODUCTION

Dielectric Loaded Accelerating (DLA) structures are emerging as a possible, important future alternative to all-metal based accelerating structures, leading to the possibility of very high accelerating gradients and more compact and cost effective accelerators. One principal effect limiting further advances in this technology is the problem of multipactor, particularly for externally powered DLA structures [1]. Unlike the well understood multipactor problem for dielectric rf windows, where the rf electric field is tangential and the rf power flow is normal to the dielectric surface, strong normal and tangential rf electric fields are present from the TM_{01} accelerating mode in DLA structures and the power flow is parallel to the surface at the dielectric-beam channel boundary. The fraction of the power absorbed at saturation in DLA experiments was found to increase with the incident power, with more than 30% of the incident power per unit length being absorbed [1]. Different TiN coating techniques including Physical Vapor Deposition (PVD) and Atomic Layer Deposition (ALD) have been tested in order to reduce the multipactor [2]. However, a significant amount of rf power loss remains, along with the accompanying emission of fluorescent light. Using geometric factors, particularly the introduction of surface

grooves may help trap the secondary electron emission in DLA structures. But success of this approach strongly depends on a few critical dimensions of the groove geometry, which leads to a very tight machining tolerance and in turn increases the fabrication difficulties and costs.

A new approach using an applied solenoid field to completely terminate multipactor in DLA structures was suggested recently [3]. The concept of using an external magnetic field to alleviate multipactor has been studied for other applications, e.g. the electron cloud in a beam chamber or high power rf windows, but the EM- field pattern of these devices and the effects of an external magnetic field are quite different from those in DLA structures. Based on a model of multipactor in DLA structures, an external DC magnetic field in the longitudinal direction is found to continuously reduce the period for secondary electrons hopping on the dielectric surface (and thus spoil the resonance condition) when the ratio of the gyro-frequency to the rf frequency (Ω/ω_{rf}) is in the range of 0.25 to 2. (The gyro-frequency, Ω , is a plasma parameter: for electrons it is defined as $\Omega = eB/m_e c = 1.76 \times 10^7 B$ rad/s, where B is the magnetic field component perpendicular to the electron motion plane). On the other hand, the multipactor is actually enhanced when the ratio is outside of this range. The optimal range to completely block multipactor is $\Omega/\omega_{rf} = 0.7 \sim 1$, equivalent to a solenoid field range from 2.8 kG to 4 kG for an X-band DLA structure. This approach is more attractive than other techniques since it can maintain all the advantages of regular DLA structures and it is independent of the accelerator parameters other than the operating frequency. Permanent magnets can also be used in place of the solenoid.

EXPERIMENT

In order to test this approach, we have developed an alumina based DLA structure and performed an experiment at Naval Research Laboratory where a 11.4 GHz 20 MW (200 ns FWHM pulsed rf) magnicon rf station was used to power the structure. The DLA structure consists of a single piece metalized alumina tube enclosed in a copper housing for a vacuum seal and two rf couplers to couple rf in and out. The upper sketch in Fig. 1 shows the geometry of the dielectric accelerator; a dielectric tapered transition is used to match the impedance between the coupler and accelerating section. The center beam channel is 8.53 mm in diameter. The ceramic material is alumina which has a dielectric

*Work supported by the Department of Energy SBIR program under Contractor #DE-SC0007629.
[#]jingchg@hep.anl.gov

constant of 9.7. The structure operates in the traveling wave TM_{01} mode, which has only three components: the electric field parallel to the axis, E_z ; the electric field normal to the dielectric surface, E_r , and the azimuthal magnetic field, H_ϕ . Figure 1 shows the normalized field amplitude of E_r and E_z along the structure. The actual gradient of the structure is 12.5 MV/m per 10 MW input power. The field profile of the external magnetic field induced by a solenoid in the experiment, B_z , is also shown.

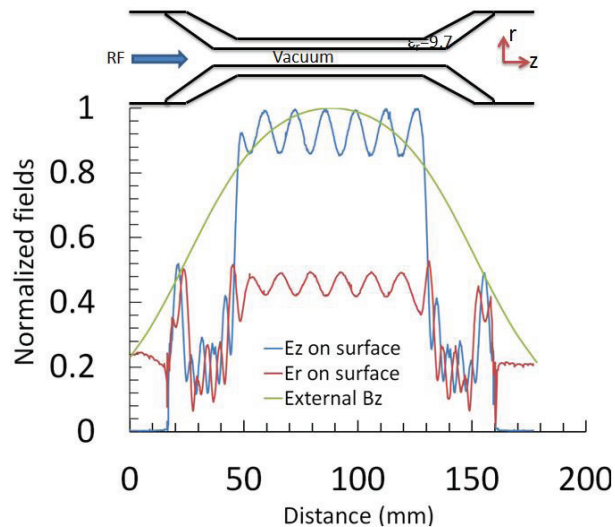


Figure 1: Sketch of the geometry, and the corresponding normalized electrical fields and external solenoid field of the alumina tube used in the experiment.

During the experiment, without an external solenoid field we observed multipactor in the DLA structure through its associated phenomena including a decrease of rf transmission and an increase of light emission while the incident rf power was increased beyond about 1 MV/m, very similar to the facts presented in [1]. When the solenoid field is applied, depending on its field strength the multipactor can be either enhanced or suppressed as shown in Fig.2. Figure 2a shows typical rf reflection signals captured through a diode detector for the external magnetic field on and off. Since the input rf pulse is Gaussian in shape we can see that, without an applied B_z , the reflection signal sharply increases at a particular threshold level of the rf field, which indicates the onset of multipactor. In the case B_z is applied, there exists a sharp reduction in the rf reflection. Meanwhile we observed the bright light accompanying the multipactor disappeared (the light image was focused on the center of DLA structure) and rf transmission was improved. Figure 2b plots rf transmission through the DLA structure while sweeping the strength of the applied solenoid for various gradients (equivalent to various input rf power levels). As predicted by theory [3], a weak solenoid field will enhance the multipactor induced rf loss, hence suppress multipactor when B_z is in the optimal range. Also Ref. [3] predicts that the multipactor would be enhanced again when B_z is increased beyond the optimal range. Limited

by the capabilities of the available solenoid, we could not verify this prediction in the experiment. In addition, the data show that a higher gradient is favorable for multipactor suppression, indicating the advantage of this approach in practical use.

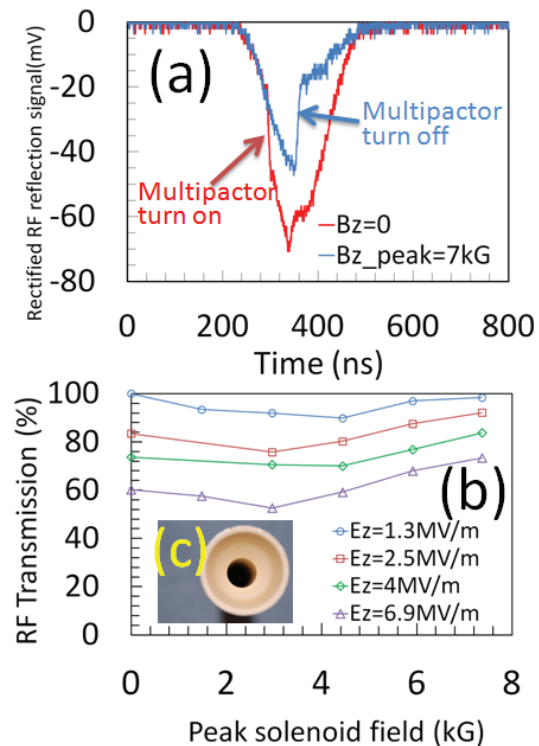


Figure 2: a) Comparison of the reflected rf signals at $E_z=4$ MV/m in the case of no external solenoid and 7 kG field applied at the center of the structure; b) Measured fraction of transmitted rf power while sweeping the strength of solenoid field for different values of E_z ; c) picture of disassembled input end of a DLA shows that an intensified multipactor occurred in the taper region of the dielectric tube.

However, note that the rf transmission was not improved to its level before the multipactor occurred. Also, the optimal value of B_z that is required to block multipactor is much larger than that given by the theoretical calculation mentioned earlier. Figure 2b shows that without the solenoid field, 40% of the rf power is absorbed when the gradient increases from ~ 1 MV/m to ~ 7 MV/m; but it is only improved by $\sim 15\%$ with the application of a 7 kG peak solenoid field. As shown in Fig.1, the non-uniformity of the applied external solenoid field along the structure (caused by a large bore to length ratio of the solenoid) resulted in a non-uniform effect on multipactor suppression during the experiment. For example, we observed complete multipactor suppression in the center section of the DLA structure when the peak value of the solenoid field was in a certain range, but multipactor in the region of the dielectric tapers, where B_z had only half of its peak value, were largely enhanced which resulted in excess rf absorption. Figure 2c shows a discolored ring at the input end of dielectric taper which

indicates where intensified electron bombardment has occurred. Higher gas pressure were also observed in the ion pumps located at near both ends of the structure while the high B_z was applied.

MODELING

For single-surface resonant multipactor, the electron experiences the normal field $E_r = (\pi a / \lambda_z) E_{rf0} \sin(\omega t + \varphi) e_r$ and tangential field $E_z = E_{rf0} \cos(\omega t + \varphi) e_z$. The first-order resonant condition is that electron flight time satisfies $\tau \sim T$, emission phase $\varphi \sim 0$, and $E_{dc} = E_r / \pi$. By applying the external $B_z = B e_z$, the trajectory and flight time of electrons are effectively altered under $E_r \times B_z$. We define the 1st electron to be the electron starting at the resonant phase $\varphi \sim 0^\circ$. With increasing Ω / ω_{rf} , ϵ_c varies non-monotonically and the flight time gradually decreases. For a given magnetic field, a higher RF field leads to a larger impact energy while the flight time doesn't change since t/τ mainly depends on Ω / ω rather than the amplitude of E_r . Since the peak for the secondary emission yield (SEY) curve is usually located at 300-400 eV, a higher energy has a lower SEY for the right branch of SEY curve. Besides, the transit time satisfies $\tau/T \sim 0.5-0.85$ for $\Omega / \omega \in (0.5, 1.5)$, and thus, within the time interval $t \in (\tau, T)$, F_r keeps pointing into the dielectric and the newly produced secondary electrons are quickly pulled back under the restoring force F_r and only attain a very low energy $\epsilon_{se} < \epsilon_1$, and very short transit time $\tau_{se} \ll T - \tau$.

During the development and saturation stage of multipactor, surface gas is desorbed, resulting in the plasma discharge in the ambient gas above the dielectric. The increase of electron density reflects the discharge delay time τ_b , $n_e = n_0 \exp(t/\tau_b)$, where n_0 is the initial density. Here, we use $\ln(n_e/n_0)$ to characterize the development of multipactor. As shown in Fig.3, with increasing B_z , variation of the electron density is non-monotonic for almost all RF field strengths. The density increases even faster and multipactor develops even more strongly at low magnetic fields compared with no magnetic field, and the density peak occurs at $B_z \sim 0.2$ T for the low RF field values $E_z = 2.5$ MV/m and $E_z = 1.3$ MV/m. With the RF field increasing, the multipactor suppression effect gradually increases as illustrated in Fig.3, since increasing the RF field is beneficial for decreasing the descendant secondary flight times and impact energies, and to increase the impact numbers. Consequently, for the method of suppressing multipactor by an external magnetic field, there is a potential to improve the power capacity significantly.

Since the external magnetic field in our experiment is non-uniform because of the short solenoid, the amplitude B_z at the breakdown area of the taper is 0.55-0.65 of the central maximum magnetic field, and there is the transverse component $B_r \sim 0.15 B_z$. Moreover, the B_z field can be decomposed into tangential and normal components (B_t, B_n) on the 17° taper. Consequently, the maximum B_n/B_t can reach 0.5 under the total effect of B_r and B_z . Furthermore, the RF field at the taper area varies

considerably. Large values of E_r and E_z are present in the breakdown ring area.

For the blue curves in Fig.3, the peak electron density for the taper occurs at total $B_z \sim 0.4$ T (amplitude in the center waveguide), corresponding to local $B_z \sim 0.2$ T in the taper. This is because the total magnetic field is lower at the taper and the electron flight time mainly depends on the magnetic field, so the electron flight time τ is higher, the remaining time $t \in (\tau, T)$ is smaller, and the multipactor suppression effect becomes weak. Moreover, the existence of a normal Ω_r generates the Lorentz forces $e u_0 \Omega_r$, $e u_t \Omega_r$, which couple the radial, angular, and longitudinal equations, leading to the influence of the

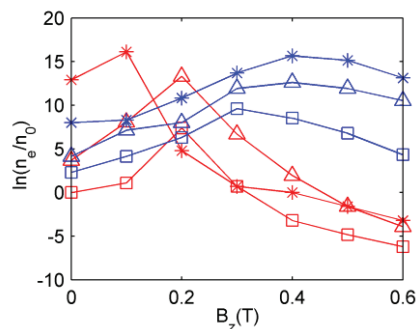


Figure 3: Variation of statistical n_e with the external magnetic field B_z and RF field E_z in the dielectric waveguide (Red curves) and in the taper (Blue curves) with $B_r = 0.5 B_t$ ('*' for $E_z = 6.9$ MV/m, 'Δ' for $E_z = 2.5$ MV/m, '□' for $E_z = 1.3$ MV/m).

tangent field E_t on the angular velocity u_0 by $e u_t \Omega_r$, and on the electron flight time and impact energy, disturbing the course of multipactor suppression. Multipactor suppression in the waveguide and multipactor strengthening at the taper compete so that the total suppression effect is partially weakened.

This analysis has also been confirmed by numerical simulation using a multipactor tracking code, SLAC Track3P (Fig.4). With an external B-field, there is strong MP occurring close to the dielectric tapers. Their resonant particle trajectories occur in the azimuthal direction.

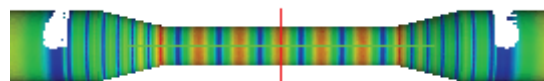


Figure 4: Numerical simulation of multipactor using the SLAC S3P and Track3P codes. Colors represent the electric field of the TM_{01} mode, and the white indicates resonant secondary electrons.

REFERENCES

- [1] J. Power, *et al*, *Phys. Rev. Lett.* 92, 164801 (2004).
- [2] C. Jing, *et al*, *IEEE Trans. Plasma Sci.* 38, 6, (2010): 1354- 1360.
- [3] C. Chang, *et al*, *J. App. Phy.*, 110, 063304 (2011).